NIH Public Access
Author Manuscript
J Nucl Cardiol. Author manuscript; available in PMC 2013 February 1.

Published in final edited form as:
J Nucl Cardiol. 2012 February ; 19(1): 100–108. doi:10.1007/s12350-011-9473-x.

Effect of Bismuth Breast Shielding on Radiation Dose and Image Quality in Coronary CT Angiography

Andrew J. Einstein, MD, PhD[a,b], **Carl D. Elliston, MA**[c], **Daniel W. Groves, MD**[a], **Bin Cheng, PhD**[d], **Steven D. Wolff, MD, PhD**[a,b,e], **Gregory D. N. Pearson, MD, PhD**[b], **M. Robert Peters, MD**[b,e], **Lynne L. Johnson, MD**[a], **Sabahat Bokhari, MD**[a], **Gary W. Johnson, AAS**[c], **Ketan Bhatia, CNMT**[a], **Theodore Pozniakoff, RT, CNMT**[a,b], and **David J. Brenner, PhD, DSc**[c]

[a]Department of Medicine, Cardiology Division, Columbia University Medical Center/New York-Presbyterian Hospital, New York, NY, USA

[b]Department of Radiology, Columbia University Medical Center/New York-Presbyterian Hospital, New York, NY, USA

[c]Center for Radiological Research, Columbia University Medical Center/New York-Presbyterian Hospital, New York, NY, USA

[d]Department of Biostatistics, Columbia University Medical Center/New York-Presbyterian Hospital, New York, NY, USA

[e]Advanced Cardiovascular Imaging, New York, NY, USA

Abstract

Background—Coronary computed tomographic angiography (CCTA) is associated with high radiation dose to the female breasts. Bismuth breast shielding offers the potential to significantly reduce dose to the breasts and nearby organs, but the magnitude of this reduction and its impact on image quality and radiation dose have not been evaluated.

Methods—Radiation doses from CCTA to critical organs were determined using metal-oxide-semiconductor field-effect transistors positioned in a customized anthropomorphic whole-body dosimetry verification phantom. Image noise and signal were measured in regions of interest (ROIs) including the coronary arteries.

Results—With bismuth shielding, breast radiation dose was reduced 46–57% depending on breast size and scanning technique, with more moderate dose reduction to the heart, lungs, and esophagus. However, shielding significantly decreased image signal (by 14.6 HU) and contrast (by 28.4 HU), modestly but significantly increased image noise in ROIs in locations of coronary arteries, and decreased contrast-to-noise ratio by 20.9%..

Conclusions—While bismuth breast shielding can significantly decrease radiation dose to critical organs, it is associated with an increase in image noise, decrease in contrast-to-noise, and changes tissue attenuation characteristics in the location of the coronary arteries.

Keywords

coronary CT angiography; radiation dose; bismuth shielding; breast shielding

Address for Correspondence: Andrew J. Einstein, MD, PhD, Telephone: 212-305-4275, Fax: 212-305-4648, andrew.einstein@columbia.edu, Mailing Address: Cardiology Division, Columbia University Medical Center, 622 West 168th Street PH 10-203A, New York, NY 10032.

Disclosures: Dr. Wolff serves as a consultant to GE Healthcare and is an owner of NeoSoft, LLC and NeoCoil, LLC. Dr. Einstein has received research grants from GE Healthcare and Spectrum Dynamics.

NIH-PA Author Manuscript
NIH-PA Author Manuscript
NIH-PA Author Manuscript

NIH-PA Author Manuscript

NIH-PA Author Manuscript

NIH-PA Author Manuscript

INTRODUCTION

Coronary computed tomography angiography (CCTA) is increasingly utilized for the noninvasive assessment of coronary artery disease due its ability to exclude or diagnose coronary artery disease with high accuracy.[1, 2] However, CCTA can be associated with high radiation doses to organs, such as the breasts and lungs, which lie in the path of the x-ray beam. When helical technique is used, absorbed doses to these critical organs have been observed to range between 42 and 91 mGy, and the attributable risks of breast and lung cancer can each exceed 0.2%.[3]

As with all medical procedures utilizing ionizing radiation, it is incumbent upon practitioners to keep radiation exposure from CCTA as low as reasonably achievable (ALARA), while still ensuring diagnostically adequate image quality. Several scanner-based approaches have been employed to significantly decrease radiation doses from CCTA, including modulating the x-ray's tube current depending on the portion of the cardiac cycle [4], step-and-shoot [5, 6], volume [7], and high-pitch helical [8] scan modes, decreasing tube potential [9], and iterative reconstruction of images.[10] Many of these dose reduction features, however, are only implemented on more recent 64+ slice CT scanners and are thus not available for a sizable portion of the installation base of CCTA-capable scanners. An alternative or additional approach to these scanner-based methods for reducing patient radiation exposure is to employ patient-based shielding.

Of particular potential appeal is the use of in-plane bismuth shielding. In-plane bismuth shielding over radiosensitive superficial organs, e.g. eyes, thyroid, and breasts, has been successfully employed for other types of CT scans. Bismuth breast shielding has been demonstrated in multiple studies to reduce radiation doses to the breasts by as much as 57% during CT examinations,[11–23] One recent study noted bismuth shielding to result in a reduction in breast dose of 38.4% in 64-slice and 46.8% in 320-slice CCTA.[24]

Thus, breast shielding is an attractive possibility for CCTA due the significant reduction in radiation doses achieved in other contexts and its ease of use. Nevertheless, a barrier to the widespread adoption of bismuth shielding in CCTA protocols is the potential increase in image noise and streak artifacts and loss of signal that may create sub-optimal examinations. Recent studies have shown mixed effects of bismuth breast shielding in CT examinations for types of examinations other than CCTA. Reflecting this discrepant data, some authors have recommended the use of shielding in non-cardiac CT [11, 13] and others have recommended against it.[15, 16] To the best of our knowledge, no previous publication has studied the effect of breast shielding on image quality in CCTA.

The purpose of this study was to determine the reduction in radiation dose to critical organs, namely the breasts, lungs, esophagus, and heart using bismuth breast shielding, and to determine how shielding affects image quality during CCTA. In addition, the effects of breast size and scanning technique (helical vs. axial step-and-shoot) on radiation dose and image quality were investigated.

MATERIALS AND METHODS

Study Design

Doses to critical organs were measured using solid-state metal-oxide-semiconductor field-effect transistor (MOSFET) radiation detectors placed in a whole-body anthropomorphic phantom. Image signal, contrast, and noise in coronary arteries was calculated using the same phantom with MOSFETs removed. Doses and image signal, contrast, and noise were

NIH-PA Author Manuscript

NIH-PA Author Manuscript

NIH-PA Author Manuscript

determined both with and without a commercially available bismuth breast shield, using both helical and axial step-and-shoot scan protocols, and for differently sized breasts.

Phantoms

A custom-adapted whole-body dosimetry verification phantom (ATOM 701; CIRS, Norfolk, Virginia) was employed. The phantom (Figure 1) is made of tissue-equivalent polymers and resins, and is both physically and radiographically similar to a human. Its height and weight are 173 cm and 73 kg, respectively, and its thoracic dimensions are 23–32 cm without breasts attached. The phantom is composed of a stack of 25 mm-thick contiguous slabs that have 5 mm-diameter holes drilled in the craniocaudal direction at positions optimized for measuring radiation doses to internal organs. MOSFETs were placed within holes corresponding to critical organs for CCTA. This phantom was modified with the addition of either medium- or large-sized tissue-equivalent breast phantoms that were constructed based on patient CT data (Figure 1). For the medium-breast phantom, two additional breast phantoms were attached to the whole-body phantom that each had an approximate volume of 385 cc. Likewise, the large-breast phantom consisted of two additional breast phantoms each with an approximate volume of 670 cc attached to the whole-body phantom. In addition, for evaluation of image signal, contrast, and noise, phantom coronary arteries were constructed and fit without gaps in holes drilled in the locations of the mid left anterior descending (LAD) coronary artery, mid left circumflex (LCx) coronary artery, and mid right coronary artery (RCA). These coronary artery phantoms were constructed as capped cylinders of soft-tissue equivalent material, with wall thickness of 0.5 mm and inner diameter of 4 mm. Coronary artery phantoms were filled with a mixture of 2.5% iohexol with 300 mg I/ml (Omnipaque, GE Healthcare, Princeton, NJ) diluted in 97.5% normal saline, a concentration determined systematically to result in “coronary” opacification during CT to levels comparable to those during clinical CCTA examinations.

MOSFET Dosimeters

A mobile MOSFET dosimetry verification system (TN-RD-70W; Best Medical, Ottawa, Canada) reader was used together with high-sensitivity MOSFET dosimeters (TN-1002RD; Best Medical). MOSFET dosimeters were calibrated using an electrometer and ionization chamber combination (Model 1015; Radcal, Monrovia, Ca), to relate voltage readout to the absorbed dose of radiation. MOSFET dosimeters were positioned within the phantom at locations corresponding to the breasts, lungs, heart, and esophagus to characterize radiation doses to these organs (Figure 2). The dosimetry system enables readout from up to 20 MOSFETs simultaneously. Since to cover the organs of interest we desired point doses at more than 20 locations, each scan was repeated five times, each with different MOSFET positioning: i)with MOSFETs placed in the lung, esophagus, and heart; ii) with MOSFETs placed in the breast, and iii) three times without MOSFETs, performed to assess image quality. The initial scans had 3, 7, and 9 MOSFETs positioned to measure radiation dose to the esophagus, lung, and heart, respectively, while the second scans had 5 MOSFETs positioned within the medium-breast phantom or 16 within the large-breast phantom.

Bismuth Breast Shielding

For the selected examinations, 4-ply bismuth shielding (AttenuRad ARB42 and ARB 53, F&L Medical Products, Vandergrift, Pennsylvania) was used to cover the medium- or large-breast phantoms that were attached to the whole-body phantom (Figure 3). The shield consisted of a 1 mm thick piece of bismuth-impregnated synthetic rubber with a 6.35 mm foam offset, and was 0.06mm lead equivalent. The foam offset was placed directly over the breast phantom with the bismuth-impregnated synthetic rubber on the anterior side.

NIH-PA Author Manuscript

NIH-PA Author Manuscript

NIH-PA Author Manuscript

CT Scans

CT examinations were performed with a 64 detector-row scanner (Lightspeed VCT XT, GE Healthcare, Waukesha, Wisconsin). A heart rate of 60 beats per minute was simulated using a "chicken heart" algorithm incorporated into the scanner's cardiac monitor. Scans were performed with tube potential of 120 kV, fixed tube current 600 mA, collimation of 64 0.625 mm, and scan length of 14 cm. A pitch of 0.2 was used for helical scans, and 100 msec of dynamic padding was used for axial step-and-shoot scans. Due to the decreased radiation doses from axial imaging, and resultant decrease in MOSFET signal-to-noise statistics, axial scans performed for dosimetry were repeated twice, with the total MOSFET voltage measured and divided by two to obtain average voltage per scan. In total, 48 CCTA scans were performed for this study, for each combination of shielding or no shielding, helical or axial (performed twice when MOSFETs placed) scanning, medium or large breast, and set of MOSFET positions (performed three times when MOSFETs not placed).

Organ Radiation Dose Calculations

Absorbed doses to the breasts, lungs, heart, and esophagus were determined for each combination of shielding or no shielding, helical or axial scanning, and medium or large breasts. The absorbed dose to an organ was calculated as the arithmetic mean of the doses for MOSFETs positioned within that organ. Dose-length product, as reported on the scanner console, was recorded for each scan protocol.

Quantitative Measures of Image Quality

Image signal and noise were determined at two levels in 5 mm^2 regions of interest within the contrast-opacified mid LAD, LCx, and RCA, using an Advantage workstation (GE Healthcare). Image signal and noise were calculated as the mean and standard deviation, respectively, of CT numbers in these regions of interest, expressed in Hounsfield units (HU). Image contrast was calculated as the mean CT number in a contrast-opacified region of interest less that in a 250 mm^2 non-contrast region of interest located approximately equidistantly between the coronary regions of interest. Image signal, contrast, and noise were determined for each of the 24 CCTAs performed without MOSFETs.

Statistical Analysis

Radiation dose was compared between shielded and unshielded scans, and between axial step-and-shoot and helical imaging, using two-tailed paired Student's t-tests. Linear mixed effects models were used in assessing the effects of shielding, breast size, and scan mode on image quality. Random subject effects were included to account for repeated measures at the three coronary artery locations. Statistical analyses were performed using Stata 11.1 (StataCorp, College Station, TX) and SAS 9.2 (SAS Institute, Inc., Cary, NC), with a p-value of ≤ 0.05 denoting statistical significance.

RESULTS

Radiation Doses

Organ absorbed doses from CCTA are summarized in Table 1. Dose-length product was 1424.5 mGy×cm for helical scanning and 351.3 mGy×cm for axial scanning. Bismuth shielding significantly decreased organ doses ($p<0.001$); a significant difference was found in both medium- and large-breast phantoms, and for both helical and axial scanning ($p<0.02$ for each). Breast dose was decreased by 46–57% with shielding, depending on the scan protocol and breast size. Doses to the lungs, heart, and esophagus were decreased more modestly with bismuth shielding. Dose reduction from axial imaging in comparison to

NIH-PA Author Manuscript

NIH-PA Author Manuscript

NIH-PA Author Manuscript

helical imaging averaged 73%; this dose reduction did not differ significantly between shielded and unshielded scans (p=0.15).

Effect on CT Attenuation Values

Average image signal and contrast for ROIs in the location of the coronary arteries are summarized in Tables 2 and 3, respectively. Average signal (i.e. average CT number, by 14.6 HU) and contrast (by 28.4 HU) were both significantly decreased with shielding (p<0.001). On a per-vessel basis, these differences between shielding and no shielding were significant for all coronary arteries (p<0.001 for LAD, LCx, and RCA).

Image Noise

Image noise is tabulated in Table 4. Image noise was modestly but significantly greater in the location of the coronary arteries with bismuth shielding than without shielding (effect of shielding 2.3 HU [6.8%], p=0.005). This increase in noise with shielding was significant for each of the coronary artery locations. Neither breast size nor scan mode was significantly associated with noise, controlling for shielding status and location. On visual inspection, no streak artifacts from the breast shields were observed in the vicinity of the coronary arteries.

Contrast-to-Noise

Contrast-to-noise ratio was significantly decreased in shielded scans by 20.9% (p<0.001). Higher contrast-to-noise ratio was observed for all coronary arteries, breast sizes, and scan modes (Table 4). Contrast-to-noise ratio decreased with shielding by 9.6 to 29.2%, depending on the artery, breast phantom, and scan mode.

DISCUSSION

Bismuth shielding has been shown in multiple studies to decrease radiation doses from CT examinations to radiosensitive superficial organs including the breast. Here, we observed bismuth breast shielding to reduce breast dose from CCTA by 46–57%, depending on breast size and scanning method, comparable to dose reductions reported previously. Absorbed dose to the heart, esophagus, and lungs was more modestly decreased with bismuth shielding, accounting to the breast's superficial location and proximity to the bismuth shield.

This significant reduction in doses was counterbalanced, however, by a worsening in quantitative measures reflecting imaging quality specifically in the area of the coronary arteries, which are the structures for which optimal image quality is critical for CCTA. Image noise increased, and contrast-to-noise ratio decreased, with shielding. Moreover, shielding changed image attenuation characteristics, decreasing CT number by ~15 HU and contrast by ~28 HU. Such altered attenuation could interfere with plaque characterization or coronary artery calcium scoring.

Previous studies evaluating the impact of bismuth shielding on radiation dose and qualitative and quantitative assessment of image quality have shown seemingly discordant results, although this to a large degree reflects different approaches to characterizing image quality. Several studies showed dose reduction without impact on image quality. For example, Hopper et al. observed, in thoracic CT, no artifact from shielding occurring more than 2 cm below the skin surface, and specifically did not visualize artifacts in the lung parenchyma or mediastinum.[11] Chang et al. found artifacts to be minimal if the distance between bismuth shielding and organs (breast, thyroid, or eye) was greater than 1 cm.[12] In a series of 50 thoracic scans, Yilmaz et al. observed no differences in image quality between shielded and unshielded lungs.[13] However, none of these studies quantitatively assessed image noise in organs being imaged. In a series of 50 pediatric chest and abdominal CT scans, Fricke et al.

NIH-PA Author Manuscript

NIH-PA Author Manuscript

NIH-PA Author Manuscript

observed no perceptible difference in image quality and no significant increase in quantitatively-assessed noise in the lungs with shielding[14], although subsequent work from the same group has shown increased noise in the region of the heart from pediatric chest CT.[22]

In contrast, several studies of non-cardiac CT have found worsening of image quality with bismuth shielding. Gelejins et al. and Vollmar and Kalendar both demonstrated beam hardening/streak artifacts as well as increased noise with shielding.[15, 16], although these artifacts were primarily in the region of the breasts rather than in diagnostic portions of the image.[15] Colombo et al. reported decreased image quality in regions immediately behind a breast shield, but not in areas of diagnostic interest for thoracic CT, and significant increase in image noise only in the anterior portions of the lung during chest CT examination.[17] Hohl et al. measured significantly increased noise in the right breast 3 cm from the surface, when shielding was used for chest CT.[18] Kalra et al. observed bismuth shielding to be associated with greater image noise and increased CT attenuation values; streak artifacts were observed at 0 and 1 cm distance between shielding and the phantom's surface, but not at 2 and 6 cm distances.[19] Using a semiquantitative scale to evaluate noise in CT pulmonary angiography, Hurwitz et al. found a significant increase in noise levels in the anterior and posterior chest wall with bismuth shielding, but no significant change in noise levels in the lung or heart.[23] Thus, our findings of significantly but modestly increased image noise, but no streak artifacts from shielding in the vicinity of the coronary arteries on visual inspection, appear to be consistent in general with this prior non-cardiac literature, with the exception of the pediatric study by Fricke et al.[14]

Bismuth shielding should only be considered if its associated dose reduction is accompanied by image quality at least as good as that which could be obtained by unshielded CT using a reduced tube current achieving equivalent dose reduction.[25] Such a quantitative comparison is difficult for CCTA, since the doses to several critical organs besides the breasts should be considered, and the relationship between tube current and quantitative measures of image quality, such as contrast-to-noise ratio for a coronary region of interest, is not a simple linear association. Accurate diagnosis with CCTA requires careful and accurate evaluation of tiny structures, viz. the coronary arteries, which constitute a small portion of the images acquired. Loss of contrast-to-noise poses a challenge to this accurate evaluation, as does a change in CT attenuation characteristics, which potentially affects plaque identification and characterization. Given our data, we avoid using bismuth breast shielding for CCTA in clinical practice, an approach in agreement with the recent SCCT Guidelines on Radiation Dose and Dose-Optimization Strategies in Cardiovascular CT.[26] A change in this practice would require data demonstrating comparable diagnostic accuracy efficacy between shielded and unshielded CCTA, in reference to gold-standard diagnosis by invasive angiography. As important as radiation dose reduction is, it should not be achieved at the cost of potentially significantly decreased diagnostic testing accuracy.

Our findings underscore the importance of validating all dose-reduction methods used in cardiac imaging, rather than just uncritically adopting lower-dose methods introduced in the CT "dose wars."[27] For example, while many groups, including ours [6], have embraced prospectively-gated CCTA, the literature supporting its diagnostic accuracy is not as robust as that for retrospectively-gated CCTA [1, 2], and one study suggests a slight reduction in diagnostic performance.[28]

Approaches that can be considered for CCTA radiation dose reduction as alternatives to bismuth shielding include electrocardiographically-synchronized tube current modulation [4], iterative noise reduction/reconstruction [10, 29, 30] with decreased tube current, reduced tube potential [9], and the various prospectively-gated scan modes.[5–8]

NIH-PA Author Manuscript

NIH-PA Author Manuscript

NIH-PA Author Manuscript

One limitation of our study is that CCTA scans were performed in anthropomorphic phantoms, not in patients, and thus the image quality evaluations are not in actual clinical scans. An interesting, though predictable, finding here is that the mean dose to the breast for the large-breast phantom was lower than that for the medium-breast phantom. This is because a larger proportion of the larger breast was outside the field of the CCTA examination, and thus received very little dose, as compared with the medium-breast geometry. This observation calls attention to an issue in using mean organ dose to calculate individual risk, specifically when the radiation dose is localized and there are variations in organ size. In such a situation, although the mean organ dose is appropriate to characterize the average risk to a large population, it may be less useful for characterizing individual risk. An alternative for estimating individual risks when the radiation exposure is localized and there is a variation in organ size, is the use of dose-volume histograms rather than mean organ dose. Dose-volume histograms characterize the dose-volume frequency distribution [31], and are often used for risk estimation in the field of radiation oncology.[32]

In conclusion, while bismuth breast shielding decreases the radiation dose from CCTA to critical organs, it is associated with an increase in image noise, loss of contrast-to-noise ratio, and change in CT attenuation characteristics. Increased attention should be given to applying and better validating scanner-based methods—such as reduced tube current and potential, prospectively-triggered scan modes, and iterative image reconstruction—that can reduce radiation exposure of patients from CCTA.

Acknowledgments

Funding: Supported by NIH grants 1R01 HL109711-01 and 5KL2 RR024157, a Nuclear Cardiology Foundation/ Covidien Research Award, and an Irving Institute for Clinical and Translational Research/Columbia University Clinical Trials Office Pilot Study Award (UL1 RR024156).

References

1. Meijboom WB, Meijs MF, Schuijf JD, et al. Diagnostic accuracy of 64-slice computed tomography coronary angiography: a prospective, multicenter, multivendor study. J Am Coll Cardiol. 2008; 52:2135–44. [PubMed: 19095130]
2. Budoff MJ, Dowe D, Jollis JG, et al. Diagnostic performance of 64-multidetector row coronary computed tomographic angiography for evaluation of coronary artery stenosis in individuals without known coronary artery disease: results from the prospective multicenter ACCURACY (Assessment by Coronary Computed Tomographic Angiography of Individuals Undergoing Invasive Coronary Angiography) trial. J Am Coll Cardiol. 2008; 52:1724–32. [PubMed: 19007693]
3. Einstein AJ, Henzlova MJ, Rajagopalan S. Estimating risk of cancer associated with radiation exposure from 64-slice computed tomography coronary angiography. JAMA. 2007; 298:317–23. [PubMed: 17635892]
4. Poll LW, Cohnen M, Brachten S, Ewen K, Modder U. Dose reduction in multi-slice CT of the heart by use of ECG-controlled tube current modulation (“ECG pulsing”): phantom measurements. 2002; 174:1500.
5. Earls JP, Schrack EC. Prospectively gated low-dose CCTA: 24 months experience in more than 2,000 clinical cases. Int J Cardiovasc Imaging. 2009; 25S2:177–87.
6. Einstein AJ, Wolff SD, Manheimer ED, et al. Comparison of image quality and radiation dose of coronary computed tomographic angiography between conventional helical scanning and a strategy incorporating sequential scanning. Am J Cardiol. 2009; 104:1343–50. [PubMed: 19892048]
7. Einstein AJ, Elliston CD, Arai AE, et al. Radiation dose from single-heartbeat coronary CT angiography performed with a 320-detector row volume scanner. Radiology. 2010; 254:698–706. [PubMed: 20177085]

NIH-PA Author Manuscript

NIH-PA Author Manuscript

NIH-PA Author Manuscript

8. Achenbach S, Marwan M, Ropers D, et al. Coronary computed tomography angiography with a consistent dose below 1 mSv using prospectively electrocardiogram-triggered high-pitch spiral acquisition. Eur Heart J. 2010; 31:340–6. [PubMed: 19897497]
9. Hausleiter J, Martinoff S, Hadamitzky M, et al. Image quality and radiation exposure with a low tube voltage protocol for coronary CT angiography results of the PROTECTION II Trial. JACC Cardiovasc Imaging. 2010; 3:1113–23. [PubMed: 21070998]
10. Gosling O, Loader R, Venables P, et al. A comparison of radiation doses between state-of-the-art multislice CT coronary angiography with iterative reconstruction, multislice CT coronary angiography with standard filtered back-projection and invasive diagnostic coronary angiography. Heart. 2010; 96:922–6. [PubMed: 20538667]
11. Hopper KD, King SH, Lobell ME, TenHave TR, Weaver JS. The breast: in-plane x-ray protection during diagnostic thoracic CT--shielding with bismuth radioprotective garments. Radiology. 1997; 205:853–8. [PubMed: 9393547]
12. Chang KH, Lee W, Choo DM, Lee CS, Kim Y. Dose reduction in CT using bismuth shielding: measurements and Monte Carlo simulations. Radiat Prot Dosimetry. 2010; 138:382–8. [PubMed: 19959602]
13. Yilmaz MH, Albayram S, Yasar D, et al. Female breast radiation exposure during thorax multidetector computed tomography and the effectiveness of bismuth breast shield to reduce breast radiation dose. J Comput Assist Tomogr. 2007; 31:138–42. [PubMed: 17259846]
14. Fricke BL, Donnelly LF, Frush DP, et al. In-plane bismuth breast shields for pediatric CT: effects on radiation dose and image quality using experimental and clinical data. AJR Am J Roentgenol. 2003; 180:407–11. [PubMed: 12540443]
15. Vollmar SV, Kalender WA. Reduction of dose to the female breast in thoracic CT: a comparison of standard-protocol, bismuth-shielded, partial and tube-current-modulated CT examinations. Eur Radiol. 2008; 18:1674–82. [PubMed: 18414873]
16. Geleijns J, Salvado Artells M, Veldkamp WJ, Lopez Tortosa M, Calzado Cantera A. Quantitative assessment of selective in-plane shielding of tissues in computed tomography through evaluation of absorbed dose and image quality. Eur Radiol. 2006; 16:2334–40. [PubMed: 16604323]
17. Colombo P, Pedroli G, Nicoloso M, Re S, Valvassori L, Vanzulli A. Evaluation of the efficacy of a bismuth shield during CT examinations. Radiol Med. 2004; 108:560–8. [PubMed: 15723002]
18. Hohl C, Wildberger JE, Suss C, et al. Radiation dose reduction to breast and thyroid during MDCT: effectiveness of an in-plane bismuth shield. Acta Radiol. 2006; 47:562–7. [PubMed: 16875333]
19. Kalra MK, Dang P, Singh S, Saini S, Shepard JA. In-plane shielding for CT: effect of off-centering, automatic exposure control and shield-to-surface distance. Korean J Radiol. 2009; 10:156–63. [PubMed: 19270862]
20. Yilmaz MH, Yasar D, Albayram S, et al. Coronary calcium scoring with MDCT: the radiation dose to the breast and the effectiveness of bismuth breast shield. Eur J Radiol. 2007; 61:139–43. [PubMed: 16962280]
21. Catuzzo P, Aimonetto S, Fanelli G, et al. Dose reduction in multislice CT by means of bismuth shields: results of in vivo measurements and computed evaluation. Radiol Med. 2010; 115:152–69. [PubMed: 20012921]
22. Coursey C, Frush DP, Yoshizumi T, Toncheva G, Nguyen G, Greenberg SB. Pediatric chest MDCT using tube current modulation: effect on radiation dose with breast shielding. AJR Am J Roentgenol. 2008; 190:W54–61. [PubMed: 18094273]
23. Hurwitz LM, Yoshizumi TT, Goodman PC, et al. Radiation dose savings for adult pulmonary embolus 64-MDCT using bismuth breast shields, lower peak kilovoltage, and automatic tube current modulation. AJR Am J Roentgenol. 2009; 192:244–53. [PubMed: 19098206]
24. Abadi S, Mehrez H, Ursani A, Parker M, Paul N. Direct quantification of breast dose during coronary CT angiography and evaluation of dose reduction strategies. AJR Am J Roentgenol. 2011; 196:W152–8. [PubMed: 21257856]
25. Geleijns J, Wang J, McCollough C. The use of breast shielding for dose reduction in pediatric CT: arguments against the proposition. Pediatr Radiol. 2010; 40:1744–7. [PubMed: 20730422]

NIH-PA Author Manuscript

NIH-PA Author Manuscript

NIH-PA Author Manuscript

26. Halliburton SS, Abbara S, Chen MY, et al. SCCT guidelines on radiation dose and dose-optimization strategies in cardiovascular CT. J Cardiovasc Comput Tomogr. 2011; 5:198–224. [PubMed: 21723512]

27. Mahesh M, Hevezi JM. Slice wars vs dose wars in multiple-row detector CT. J Am Coll Radiol. 2009; 6:201–2. [PubMed: 19248997]

28. Pontone G, Andreini D, Bartorelli AL, et al. Diagnostic accuracy of coronary computed tomography angiography: a comparison between prospective and retrospective electrocardiogram triggering. J Am Coll Cardiol. 2009; 54:346–55. [PubMed: 19608033]

29. Leipsic J, Labounty TM, Heilbron B, et al. Adaptive statistical iterative reconstruction: assessment of image noise and image quality in coronary CT angiography. AJR Am J Roentgenol. 2010; 195:649–54. [PubMed: 20729442]

30. Bittencourt MS, Schmidt B, Seltmann M, et al. Iterative reconstruction in image space (IRIS) in cardiac computed tomography: initial experience. Int J Cardiovasc Imaging. 2010

31. Drzymala RE, Mohan R, Brewster L, et al. Dose-volume histograms. Int J Radiat Oncol Biol Phys. 1991; 21:71–8. [PubMed: 2032898]

32. Koh ES, Tran TH, Heydarian M, et al. A comparison of mantle versus involved-field radiotherapy for Hodgkin's lymphoma: reduction in normal tissue dose and second cancer risk. Radiat Oncol. 2007; 2:13. [PubMed: 17362522]

NIH-PA Author Manuscript

NIH-PA Author Manuscript

NIH-PA Author Manuscript

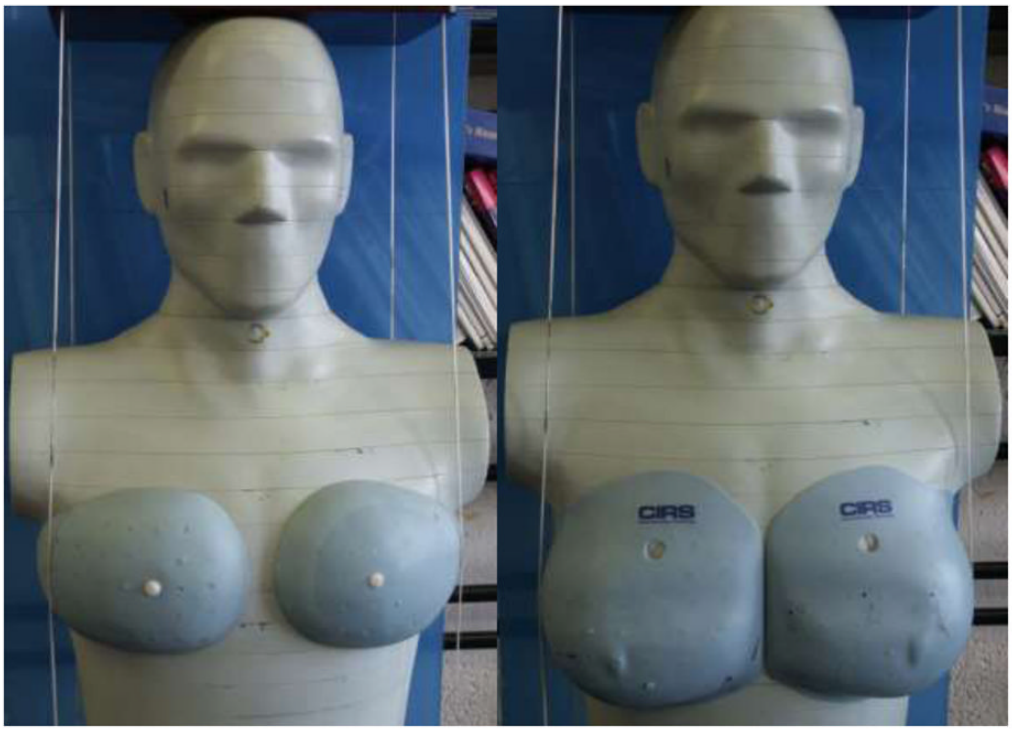

Figure 1.
Modified physical anthropomorphic phantom with medium-sized (left) and large sized (right) breast phantoms attached.

NIH-PA Author Manuscript
NIH-PA Author Manuscript
NIH-PA Author Manuscript

Figure 2.
Phantom with MOSFETs attached to measure radiation doses to internal organs during CCTA. Here, MOSFETs are positioned both in breasts and internal organs for illustrative purposes.

NIH-PA Author Manuscript

NIH-PA Author Manuscript

NIH-PA Author Manuscript

Figure 3.
Phantom positioned on a scanner with bismuth breast shield in place. MOSFET detectors can be observed emerging from below shield in the upper right hand corner.

NIH-PA Author Manuscript
NIH-PA Author Manuscript
NIH-PA Author Manuscript

Table 1

Organ Absorbed Doses (mGy) to Critical Organs from CCTA Examinations.

		Helical Scan			Axial Scan		
		No Shielding	**Shielding**	**% Reduction**	**No Shielding**	**Shielding**	**% Reduction**
Large Breast	Breast	67.5	36.4	46.1	21.3	10.3	51.7
	Lung	78.8	69.1	12.3	21.5	16.1	24.9
	Heart	100.5	70.0	30.3	26.6	18.8	29.4
	Esophagus	66.3	61.1	7.8	13.9	15.3	−10.4
Medium Breast	Breast	89.1	43.7	50.9	32.0	13.7	57.3
	Lung	78.1	63.2	19.1	20.0	16.0	20.0
	Heart	94.4	75.6	19.9	26.5	19.0	28.4
	Esophagus	61.3	57.2	6.6	15.7	13.1	16.8

NIH-PA Author Manuscript
NIH-PA Author Manuscript
NIH-PA Author Manuscript

Table 2

Image Signal in Locations of Coronary Arteries (Mean CT number in Region of Interest, Hounsfield Units)

		Helical Scan			Axial Scan		
		No shielding	**Shielding**	**Difference**	**No shielding**	**Shielding**	**Difference**
Large breast	LAD	345.5	330.6	14.9	340.2	328.4	11.8
	LCx	347.3	334.0	13.3	345.0	333.4	11.6
	RCA	394.6	389.2	5.4	390.4	380.9	9.5
Medium breast	LAD	348.4	320.2	28.2	349.3	330.2	19.1
	LCx	367.9	351.5	16.4	364.9	354.6	10.3
	RCA	363.5	345.9	17.6	366.2	349.2	17.0

NIH-PA Author Manuscript
NIH-PA Author Manuscript
NIH-PA Author Manuscript

Table 3

Image Contrast (Hounsfield Units)

		Helical Scan			Axial Scan		
		No shielding	**Shielding**	**Difference**	**No Shielding**	**Shielding**	**Difference**
Large breast	LAD	322.2	290.4	31.8	316.4	289.9	26.5
	LCx	324.0	293.8	30.2	321.1	295.0	26.1
	RCA	371.4	349.1	22.3	366.5	342.4	24.1
Medium breast	LAD	325.4	286.2	39.2	325.8	293.8	32.0
	LCx	344.9	317.5	27.4	341.4	318.1	23.3
	RCA	340.5	311.9	28.6	342.7	312.8	29.9

NIH-PA Author Manuscript
NIH-PA Author Manuscript
NIH-PA Author Manuscript

Table 4

Image Noise in Locations of Coronary Arteries (Standard deviation of CT number in Region of Interest).

		Helical Scan			Axial Scan		
		No shielding	**Shielding**	**% Increase**	**No Shielding**	**Shielding**	**% Increase**
Large breast	LAD	39.3	43.5	10.6	34.5	40.3	17.1
	LCx	29.9	33.1	10.9	38.0	32.5	−14.4
	RCA	32.5	36.0	10.7	32.6	35.8	9.9
Medium breast	LAD	30.4	33.3	9.7	38.4	36.3	−5.5
	LCx	35.2	31.4	−10.7	30.0	36.3	21.2
	RCA	33.9	42.3	24.5	37.9	39.6	4.6

NIH-PA Author Manuscript
NIH-PA Author Manuscript
NIH-PA Author Manuscript

Table 5

Contrast-to-Noise Ratios.

		Helical Scan			Axial Scan		
		No shielding	**Shielding**	**% Decrease**	**No shielding**	**Shielding**	**% Decrease**
Large breast	LAD	10.5	8.5	19.1	9.9	7.2	27.6
	LCx	12.3	9.5	22.5	9.9	9.0	9.6
	RCA	13.1	11.1	14.8	12.4	9.0	27.1
Medium breast	LAD	11.4	9.1	20.2	10.1	8.0	20.5
	LCx	11.7	10.1	13.6	11.9	9.4	21.2
	RCA	12.4	8.7	29.2	10.5	7.9	24.3